Article

A Theoretical Study on the Photochemical Isomerization of 2,6-Dimethylpyrazine

Maurizio D'Auria (ID)

Dipartimento di Scienze, Università della Basilicata, V.le dell'Ateneo Lucano 10, 85100 Potenza, Italy; maurizio.dauria@unibas.it; Tel.: +39-0971-205480

Abstract: DFT calculations on the photoisomerization of 2,6-dimethylpyrazine allowed us to confirm the role of benzvalene isomers in the isomerization of hexatomic heterocyclic compounds. 2,6-Dimethylpyrazine in the excited singlet states can be converted into the corresponding Dewar isomers. If the S_2 state is populated, two Dewar isomers can be obtained, while the S_1 state allows the formation of only one of the possible Dewar isomers. Both Dewar isomers can be converted into the benzvalene isomer, that is, the precursor of 4,5-dimethylpyrimidine, the reaction product. In fact, the benzvalene isomer can be obtained from the Dewar isomers in processes that occur without an activation energy, and it is the more stable benzvalene isomers that can be obtained from the Dewar isomers. CASSCF study indicates the presence of a conical intersection allowing the direct formation of the benzvalene isomer.

Keywords: pyrazine; photochemical isomerization; DFT; CASSCF

1. Introduction

The photoisomerization of hexatomic heterocyclic compounds is an important research field, able to give, in some cases, noticeable synthetic procedures [1–4]. In order to explain the observed reactivity, several mechanistic hypotheses have been formulated. In this way, Dewar aromatic compounds, azaprefulvene intermediates, benzvalene intermediates, aziridines, and azaprismane intermediates, have been postulated in the reaction of this type of compounds. Figure 1 collects some of these mechanistic hypotheses.
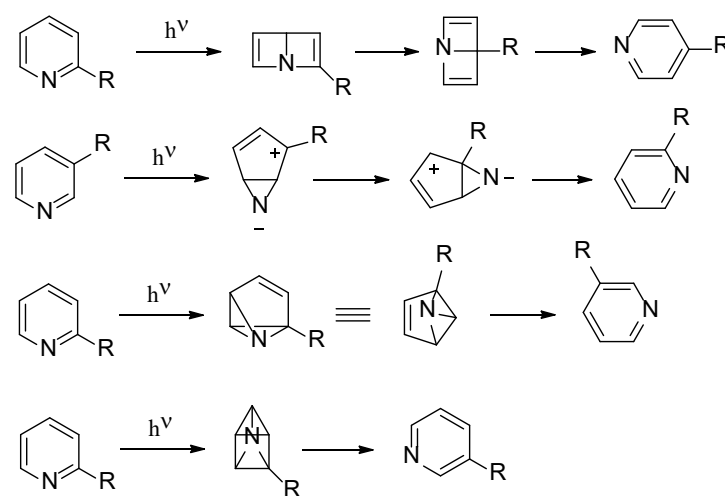

Figure 1. Proposed photoisomerization routes for hexatomic heterocycles.

In this study, we want to present the results of DFT and CASSCF study on the photochemical isomerization of 2,6-dimethylpyrazine.

2. Materials and Methods

Gaussian09 has been used for the discussions about the computed geometries [5]. All the computations were based on the Density Functional Theory (DFT) [6] and Time-Dependent DFT (TD-DFT) [7,8] by using the B3LYP hybrid xc functional [9]. Geometry optimizations and TD-DFT results from the Gaussian09 program have been obtained at the B3LYP/6-311G+(d,p) level of approximation. Geometry optimizations were performed with default settings on geometry convergence (gradients and displacements), integration grid and electronic density (SCF) convergence. Redundant coordinates were used for the geometry optimization as produced by the Gaussian09 program. Analytical evaluation of the energy second derivative matrix w.r.t. Cartesian coordinates (Hessian matrix) at the B3LYP/6-311G+(d,p) level of approximation confirmed the nature of minima on the energy surface points associated with the optimized structures. The transition states were calculated in S0 state.

Some computations were based on the Complete Active Space Multiconfiguration Self-Consistent Field (CASSCF) [10–18]. Geometry optimizations from the Gaussian09 program have been obtained at the CASSCF(6,6)/6-31G(d,p) level of approximation. Geometry optimizations were performed with default settings on geometry convergence (gradients and displacements), integration grid and electronic density (SCF) convergence.

3. Results and Discussion

The vapor phase isomerization of 2,6-dimethylpyrazine (**1**) has been described several years ago, showing that the only detectable product was 4,5-dimethylpyrimidine (**3**) (Scheme 1) [19]. To explain the observed behavior, a benzvalene intermediate had been postulated (Scheme 1). In fact, the possible isomerization of the corresponding Dewar isomers cannot be used to justify the observed reaction product (Scheme 2). Some years ago, a study appeared where, on the basis of a CASSCF study, the direct conversion of **1** into **3** without the presence of any intermediate, has been proposed [20,21].

We performed both DFT and CASSCF calculations on the above-described reaction, in order to explain the observed reactivity (Table 1). 2,6-Dimethylpyrazine shows in methanol UV absorptions at $\lambda = 208$ (592 kJ mol^{-1}) and 277 nm (432 kJ mol^{-1}) [22]. TD-DFT calculations at B3LYP/6-31G+(d,p) level of theory on Gaussian 09 gave an absorption in the gas phase at $\lambda = 242$ nm (495 kJ mol^{-1}), due to a NHOMO-LUMO $\pi \rightarrow \pi^*$ transition, and a n$\rightarrow \pi^*$ transition (HOMO-LUMO transition) at 329 nm (363 kJ mol^{-1}). Calculations at CASSCF(6,6)/6-31G(d,p) level of theory on Gaussian 09 gave an absorption in the gas phase at $\lambda = 183$ nm (654 kJ mol^{-1}), and at 217 nm (553 kJ mol^{-1}). The possible evolution of the singlet excited states calculated at DFT level of theory has been described in Figure 2.

Both S$_1$ and S$_2$ states can evolve to give the corresponding triplet state; however, that does not play an important role in the reactivity of the pyrazine derivative. The S$_2$ state can be converted into the corresponding Dewar isomer **4** and **5** (Figure 3).
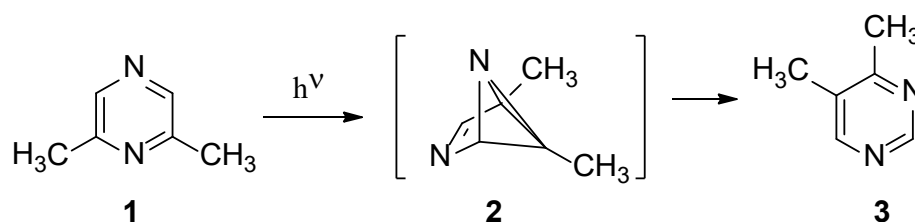
Scheme 1. Photoisomerization of 2,6-dimethylpyrazine.
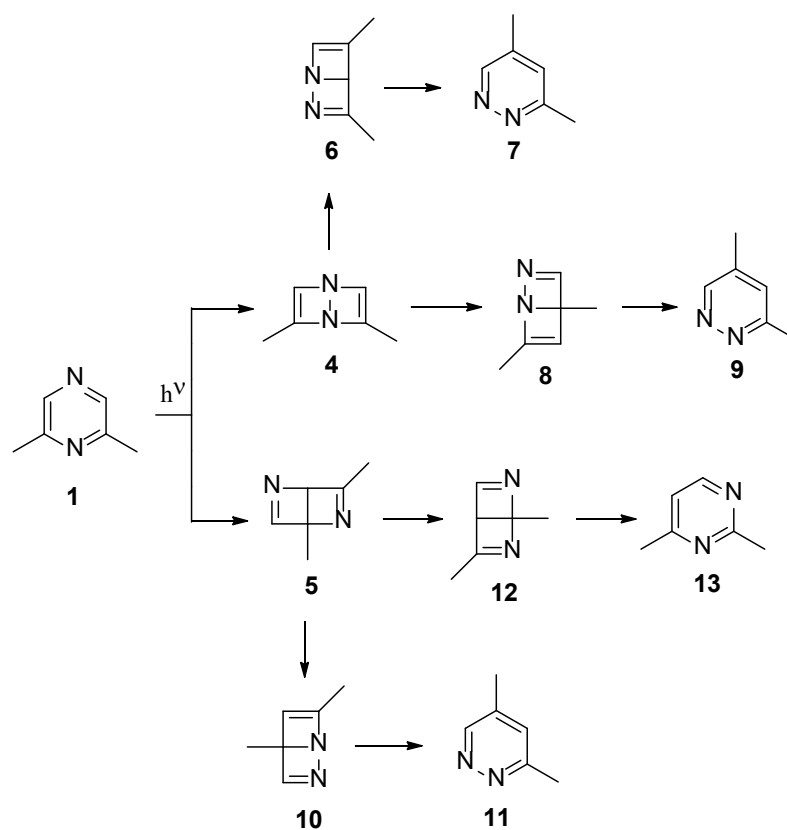
Scheme 2. Possible isomerization reactions of the Dewar 2,6-dimethylpyrazine isomers.
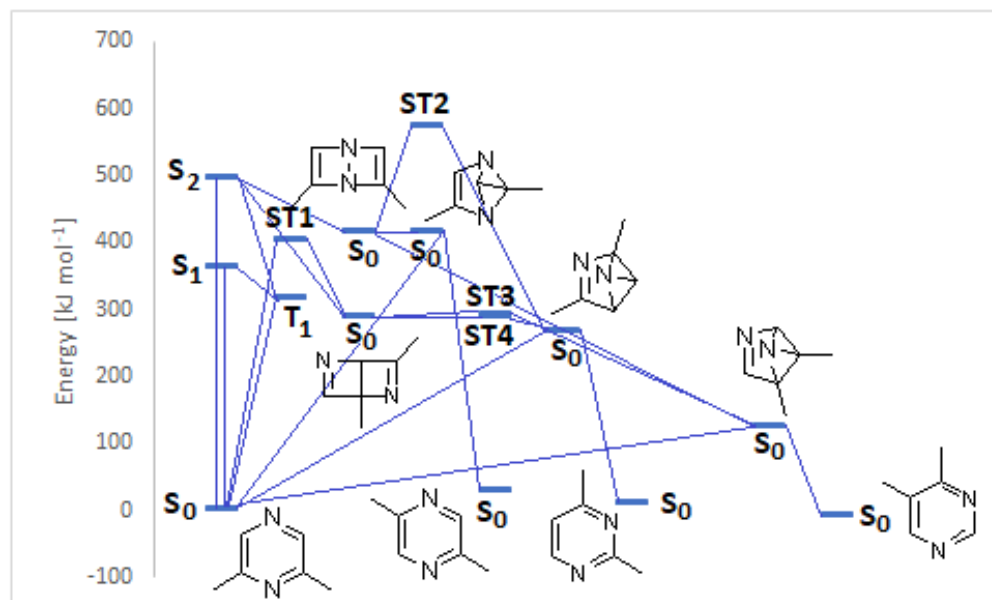

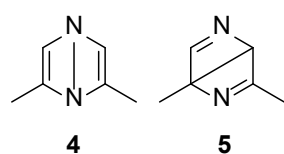**Figure 2.** Photochemical isomerization of 2,6-dimethylpyrazine.

Figure 3. Dewar isomers in the photoisomerization of 2,6-dimethylpyrazine.

Table 1. Total energy of the optimized structures.

Compound	Energy [H]
1	−342.98486740
4	−342.82721911
5	−342.8747959
14	−342.82708190
15	−342.8835509
2	−342.9375535
16	−342.8744626
13	−342.9818826
3	−342.9885549
ST1	−342.9843104
ST2	−342.8314078
ST3	−342.7664741
ST4	−342.8747059

The Dewar isomer **4** can be interconverted into the starting material in a step without a transition state, showing that this isomer has a very short lifetime. On the contrary, the conversion of the Dewar isomer **5**, which can be obtained from S_2 but also from S_1 excited singlet state, into 2,6-dimethylpyrazine necessitates overcoming a transition state with $\Delta E = 105$ kJ mol^{-1} (ST1, Figure 2).

The Dewar isomer **4** could be converted in a step without a transition state into the benzvalene intermediate **14** that showed the same energy as **4** (Figure 2 and Scheme 3). Furthermore, the Dewar isomer **4** can be converted into the benzvalene isomer **15** (Figure 2 and Scheme 3), but this step showed a transition state of 159 kJ mol^{-1} (ST2, Figure 2). Finally, **4** can be converted, without a transition state into the benzvalene isomer **2** (Figure 2 and Scheme 3). Considering the energy level of all the possible benzvalene isomers, the formation of **2** is clearly favored.
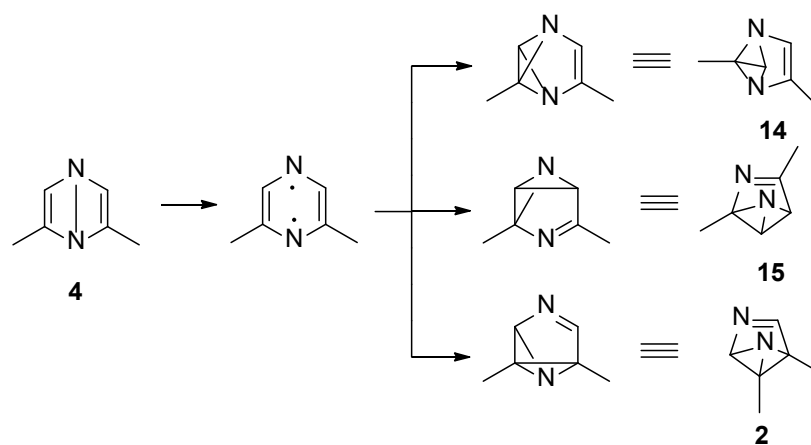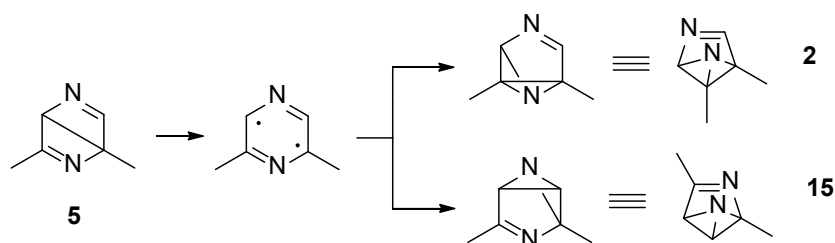

Scheme 3. Benzvalene isomers from **4**.

Scheme 4 collects the possible rearomatization reactions of the benzvalene intermediates **2**, **14**, and **15**. In red the broken bonds are evidenced. The aromatization reactions occurred without a transition state. Benzvalene **14** can give 2,5-dimethylpyrazine (**16**), while **15** can be transformed into 2,4-dimethylpyrimidine (**13**). All these compounds were not found in the reaction mixture. Only benzvalene **2**, the isomer showing the lowest energy, can be converted into 4,5-dimethylpyrimidine (**3**), the observed reaction product. This scheme is in agreement with the observed reactivity.
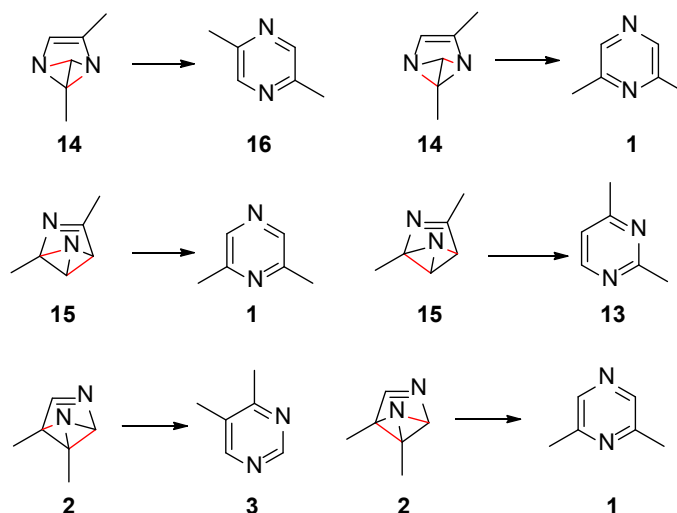
Scheme 4. Rearomatization processes of benzvalene isomers.

Both the excited singlet states of 2,6-dimethylpyrazine (**1**) can allow the formation of the Dewar isomer **5**. This isomer can return to the starting material, but this step has an activation energy of 105 kJ mol^{-1} (ST1, Figure 2). The Dewar isomer **5** can be a precursor of several benzvalene isomers (Scheme 5). In particular, benzvalene isomer **2** and **15** can be obtained.

Scheme 5. Benzvalene isomers from **5**.

The formation of **2** and **15** from **5** does not require high transition state. The conversion of **5** into **15** showed a transition energy of 1 kJ mol^{-1}, while that of **5** into **2** has a transition state at 2 kJ mol^{-1} (Figure 4). This is an early transition state with a structure similar to the starting material. Additionally, in this case, the formation of **2** is favored considering that it is the most stable compound. The low value of the transition states energy could be in agreement with the transposition nature of the reaction. Furthermore, we consider that two sp^2 carbon atoms in a cyclobutene ring disappeared, and also the other cyclobutene ring was not present in the products.

On the other hand, the CASSCF study offers a completely different possible evolution of the first excited singlet state. The results we obtained are summarized in Figure 5.

In this case, we can observe a conical intersection that allows the direct formation of **2**. The benzvalene isomer **2** can be converted into the product, on the basis of the process described in Scheme 4, with a transition state (TS2) with an energy barrier of 153 kJ mol^{-1}.

The structure of the compound at the conical intersection is reported in Figure 6.
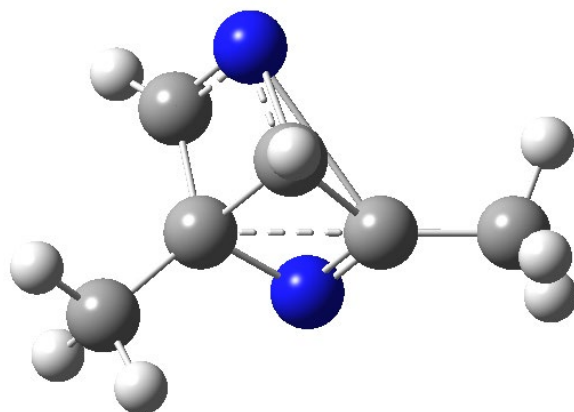
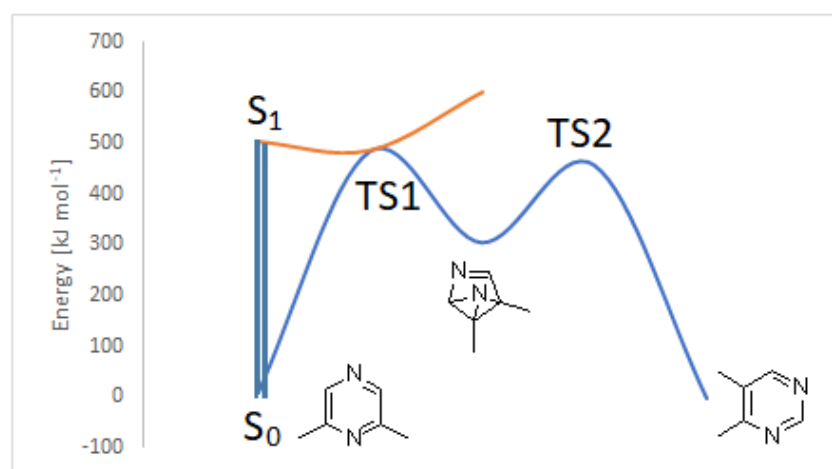**Figure 4.** Transition state of the conversion of **5** into **2**.

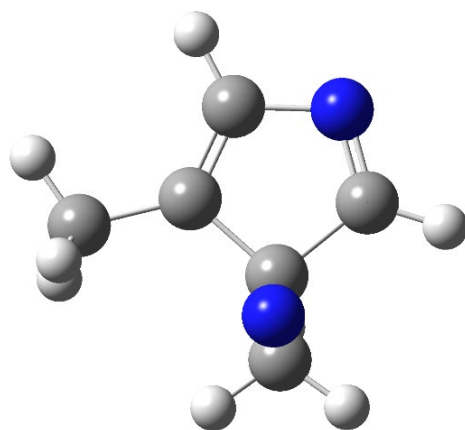**Figure 5.** CASSCF evolution of the singlet excited state of 2,6-dimethylpyrazine.

Figure 6. Structure of 2,6-dimethylpyrazine at the conical intersection.

4. Conclusions

DFT calculations allow us to present a complete description of the reactivity of 2,6-dimethylpyrazine. This compound, in the excited singlet states, can be converted into the corresponding Dewar isomers. If the S_2 state is populated, both Dewar isomers can be obtained, while S_1 state allowed the formation of only the Dewar isomer **5**. Both Dewar isomers can be converted into the benzvalene isomer **2**, which is the precursor of 4,5-dimethylpyrimidine, the reaction product. The CASSCF study proposed a very different scenario, where a conical intersection from the S_1 state allowed the direct formation of **2**.

References

1. Pavlik, J.M. Photoisomerization of some nitrogen-containing hetero-aromatic compounds. In *CRC Handbook of Organic Photochemistry and Photobiology*, 2nd ed.; Horspool, W., Lenci, F., Eds.; CRC Press: Boca Raton, FL, USA, 2004; pp. 97.1–97.22.
2. Albini, A.; Fagnoni, M. Photochemistry of N-oxides. In *CRC Handbook of Organic Photochemistry and Photobiology*, 2nd ed.; Horspool, W., Lenci, F., Eds.; CRC Press: Boca Raton, FL, USA, 2004; pp. 99.1–99.21.
3. Mariano, P.S. A new look at pyridinium salt photochemistry. In *CRC Handbook of Organic Photochemistry and Photobiology*, 2nd ed.; Horspool, W., Lenci, F., Eds.; CRC Press: Boca Raton, FL, USA, 2004; pp. 100.1–100.10.
4. Klán, P.; Wirz, J. *Photochemistry of Organic Compounds*; John Wiley & Sons Ltd.: Chichester, UK, 2009; pp. 276–279.
5. Frisch, M.J.; Trucks, G.W.; Schlegel, H.B.; Scuseria, G.E.; Robb, M.A.; Cheeseman, J.R.; Scalmani, G.; Barone, V.; Mennucci, B.; Petersson, G.A.; et al. *Gaussian 09, Revision A.1*; Gaussian, Inc.: Wallingford, CT, USA, 2009.
6. Parr, R.G.; Yang, W. *Density Functional Theory of Atoms and Molecules*; Oxford University Press: Oxford, UK, 1989.
7. Casida, M.E. Time-dependent density-functional response theory for molecules. In *Recent Advances in Density Functional Methods*; Chong, D.P., Ed.; World Scientific: Singapore, 1995; Volume 1, pp. 155–192.
8. Casida, M.E.; Jamorski, C.; Casida, K.C.; Salahub, D.R. Molecular excitation energies to high-lying bound states from time-dependent density-functional response theory: Characterization and correction of the time-dependent local density approximation ionization threshold. *J. Chem. Phys.* **1998**, *108*, 4439–4449. [CrossRef]
9. Becke, A.D. Molecular excitation energies to high-lying bound states from time-dependent density-functional response theory: Characterization and correction of the time-dependent local density approximation ionization threshold. *J. Chem. Phys.* **1993**, *98*, 5648–5652. [CrossRef]
10. Hegarty, D.; Robb, M.A. Application of unitary group-methods to configuration-interaction calculations. *Mol. Phys.* **1979**, *38*, 1795–1812. [CrossRef]
11. Eade, R.H.A.; Robb, M.A. Direct minimization in MC SCF theory—The Quasi-Newton method. *Chem. Phys. Lett.* **1981**, *83*, 362–368. [CrossRef]
12. Schlegel, H.B.; Robb, M.A. MC SCF gradient optimization of the H2CO → H2 + CO transition structure. *Chem. Phys. Lett.* **1982**, *93*, 43–46. [CrossRef]
13. Bernardi, F.; Bottini, A.; McDougall, J.J.W.; Robb, M.A.; Schlegel, H.B. MCSCF gradient calculation of transition structures in organic reactions. *Faraday Symp. Chem. Soc.* **1984**, *19*, 137–147. [CrossRef]
14. Frisch, M.J.; Ragazos, I.N.; Robb, M.A.; Schlegel, H.B. An Evaluation of 3 Direct MC-SCF Procedures. *Chem. Phys. Lett.* **1992**, *189*, 524–528. [CrossRef]
15. Yamamoto, N.; Vreven, T.; Robb, M.A.; Frisch, M.J.; Schlegel, H.B. A Direct Derivative MC-SCF Procedure. *Chem. Phys. Lett.* **1996**, *250*, 373–378. [CrossRef]
16. Siegbahn, P.E.M. A new direct CI method for large CI expansions in a small orbital space. *Chem. Phys. Lett.* **1984**, *109*, 417–423. [CrossRef]
17. Robb, M.A.; Niazi, U. The Unitary Group Approach to Electronic Structure Computations. In *Reports in Molecular Theory*; Weinstein, H., Náray-Szabó, G., Eds.; CRC Press: Boca Raton, FL, USA, 1990; Volume 1, pp. 23–55.
18. Klene, M.; Robb, M.A.; Frisch, M.J.; Celani, P. Parallel implementation of the CI-vector evaluation in full CI/CAS-SCF. *J. Chem. Phys.* **2000**, *113*, 5653–5665. [CrossRef]
19. Lahmani, F.; Ivanoff, N. Photoisomerization of pyrazine and of its methylderivatives. *Tetrahedron Lett.* **1967**, *8*, 3913–3917. [CrossRef]
20. Su, M.-D. CASCSF Study on the photochemical transposition reactions of pyrazines. *J. Phys. Chem. A* **2006**, *110*, 9420–9428. [CrossRef] [PubMed]
21. D'Auria, M. The photochemical isomerization of hexatomic heterocyclic compounds. *Curr. Org. Chem.* **2021**, *25*, 1659–1685. [CrossRef]
22. Available online: https://spectrabase.com/spectrum/JGriPcJDFzk (accessed on 10 January 2022).